

Integrated Structural Analysis and Design Using Three-Dimensional Finite Elements

B. Barthelemy,* R. T. Haftka,† U. Madapur,‡ and S. Sankaranarayanan§
Virginia Polytechnic Institute and State University, Blacksburg, Virginia 24061

A design approach that combines iterative structural analysis with a traditional iterative optimization algorithm is applied to the optimum design of the shape of a hole in a plate in tension. The plate is modeled by three-dimensional finite elements, and an element-by-element preconditioned conjugate gradient iterative algorithm is used for solving the equations of equilibrium. Several parameterizations of the optimum shape are considered, and it is shown that a sine series can describe the optimum shape with only three design variables, whereas other series require seven variables for similar results. The optimum shape compares well with an experimental optimum obtained by A. J. Durelli. An investigation is performed to determine the best way of obtaining finite-difference derivatives of the stresses with respect to design variables. It is shown that a method based on modifying the equations of equilibrium for the perturbed problem performs best. The benefit of the integrated approach is determined by comparing convergence with different initial iterates for the displacement field. It is shown that using the final iterate of the previous solution can reduce the number of analysis iterations by about 40% compared to starting with a zero initial iterate.

Introduction

ORIGINALLY, structural optimization was based on the calculus of variations; a typical problem was handled by obtaining the Euler-Lagrange optimality differential equations and solving them simultaneously with the differential equations of the structural response. More recently, nested approaches have become the standard for structural optimization. In these approaches the structural response is calculated for a given set of design variables, and derivatives of the response with respect to design parameters are used in directing the optimization search and updating the design parameters. One of the reasons for the popularity of the nested approach is that the structural analysis equations are usually solved by techniques that are quite different from those used for the design optimization.

When the structural analysis is iterative, it seems reasonable to attempt to integrate the analysis and optimization iterations. In the 1960s Fox and Schmit and their students¹ tried to integrate structural analysis and design by using conjugate gradient (CG) minimization techniques for solving linear structural analysis problems. They found that the optimization methods were not competitive with the traditional direct Gaussian elimination techniques for solving structural analysis problems. The difficulty they encountered was due to the inherent ill-conditioning of the discretized equations of equilibrium, which results in extremely slow convergence for the CG method.

More recently, preconditioned conjugate gradient (PCG) methods were developed that are competitive with elimination

techniques for poorly banded problems. The element-by-element (EBE) PCG method^{2,3} preconditions the CG method by developing an approximate inverse of the stiffness matrix that requires only the factorization of element matrices. The EBE PCG method was used for three-dimensional truss minimum mass design problems^{4,5} in an approach called simultaneous analysis and design, where the design variables include both structural sizes and the nodal displacements. The equations of equilibrium are not solved for the displacements but instead are used as equality constraints. For these problems the simultaneous analysis and design approach was shown to be superior to the nested approach. However, even though preconditioning alleviates the problems associated with the ill-conditioned equations of equilibrium, the efficiency of the simultaneous analysis and design approach still appears to be sensitive to the choice of tuning parameters for the EBE procedure as well as for the optimization procedure.

An alternative approach for integrating analysis and design was proposed by Rizk⁶ for aerodynamic design problems. Aerodynamic response is typically calculated by iterative procedures, and the integration of the analysis and design is achieved by performing only a small number of analysis iterations at each design cycle. However, this small number of iterations is chosen so that meaningful information on required design changes can be obtained from the approximate unconverged response.

The method could be applicable to structures when iterative solution methods are computationally competitive with direct methods such as Gaussian elimination. The purpose of the present work is to test the application of Rizk's approach to structural design in the linear range, when the EBE PCG method is used to solve the equations of equilibrium. Because iterative analysis techniques are particularly appropriate for three-dimensional problems, a thick plate modeled with three-dimensional finite elements was selected. The main issues addressed in the research were 1) the number of analysis iterations sufficient for convergence of the optimization procedure; 2) the best method for calculating derivatives of the approximate response with respect to design variables; and 3) the overall computational performance of the algorithm.

The design problem was also selected to be of interest on its own merits aside from its role as a test problem. It is the design of the optimal shape of a hole in a plate under uniaxial loading. The problem was solved experimentally by Durelli

Presented as Paper 89-1309 at the AIAA 30th Structures, Structural Dynamics, and Materials Conference, Mobile, AL, April 3-5, 1989. Received July 24, 1989; accepted for publication Feb. 23, 1990. Copyright © 1989 by the American Institute of Aeronautics and Astronautics, Inc. All rights reserved.

*Department of Aerospace and Ocean Engineering; currently Senior Research Engineer at Ford Motor Co.

†Christopher Kraft Professor, Department of Aerospace and Ocean Engineering. Member AIAA.

‡Department of Aerospace and Ocean Engineering; currently at H K & S, Inc., Providence, RI.

§Graduate Research Assistant, Department of Aerospace and Ocean Engineering. Student Member AIAA.

Table 1 Comparison of EBE PCG iterative solver and LDL direct solver

No. of layers	No. of elements	No. of iterations	No. of operations EBE-PCG, million FLOPS	Number of DOF, n	Bandwidth, N	No. of operations LDL ^T , million FLOPS
1	214	186	45	1488	78	4.5
2	428	147	72	2232	111	13.8
3	642	120	88	2976	144	30.9
4	856	115	113	3720	177	58.3
5	1070	103	127	4464	210	105.0
10	2140	111	273	8184	375	588.0

and Rajaiah,⁷ and it was of interest to match the analytical and experimental optima.

EBE PCG Method

The equations of equilibrium of a structure discretized by a finite element model are typically written as

$$Ku = f \quad (1)$$

where K is the stiffness matrix obtained by assembly of element matrices, u the displacement vector, and f the force vector. The matrix K is a $n \times n$ symmetric, positive-definite matrix, where n is the number of structural degrees of freedom. Equation (1) can be solved directly using Gaussian elimination or iteratively.

CG methods solve Eq. (1) by minimizing a function $\phi(u)$ so that the value of u at which $\phi(u)$ is minimum is given by $K^{-1}f$. When K is positive definite, one such function is given by

$$\phi(u) = \frac{1}{2}u^TKu - u^Tf \quad (2)$$

CG methods minimize ϕ along a set of directions conjugate (orthogonal to one another) with respect to K .

In structural problems the stiffness matrix usually has a high condition number, and the convergence of iterative methods can be improved by preconditioning K . PCG methods replace Eq. (1) by

$$BKu = Bf \quad (3)$$

where B is an appropriate inverse of K that is inexpensive to calculate. The matrix BK is then close to the unit matrix I and has a better condition number than K .

The EBE method^{2,3} starts by scaling the equations of equilibrium as

$$\bar{K}\bar{u} = \bar{f} \quad (4)$$

so that the diagonal elements of \bar{K} are all ones. We then write \bar{K} as

$$\bar{K} = I + \sum_{i=1}^{nele} k^i \quad (5)$$

where k^i is the contribution of the i th finite element to the off-diagonal part of \bar{K} and can be obtained by simple operations on the element stiffness matrix, and $nele$ is the number of elements. Finally, assuming that the elements of the k^i are small compared to 1, we approximate \bar{K} as

$$\bar{K} \cong \prod_{i=1}^{nele} (I + k^i) \quad (6)$$

Since \bar{K} is written as the product of element matrices, its inverse can be calculated by factorizing element matrices 1 by

1. The approximate inverse of K can then be obtained by scaling \bar{K}^{-1} . The EBE PCG algorithm therefore does not require a global stiffness matrix and is particularly suitable to three-dimensional problems where K is poorly banded. For such problems Gaussian elimination can require a lot of memory and CPU time.

Hole Shape Optimization Problem

The optimization problem considered here is to determine the shape of the central hole in a plate subjected to uniform loading (Fig. 1a) to minimize the stress concentration in the plate. The plate was optimized experimentally by Durelli and Rajaiah⁷ using a photoelastic technique. The dimensions shown in Fig. 1 are chosen to match their experiments. The plate is modeled by eight-node isoparametric three-dimensional finite elements; only a quarter of the plate is considered because of symmetry, and appropriate boundary conditions are applied.

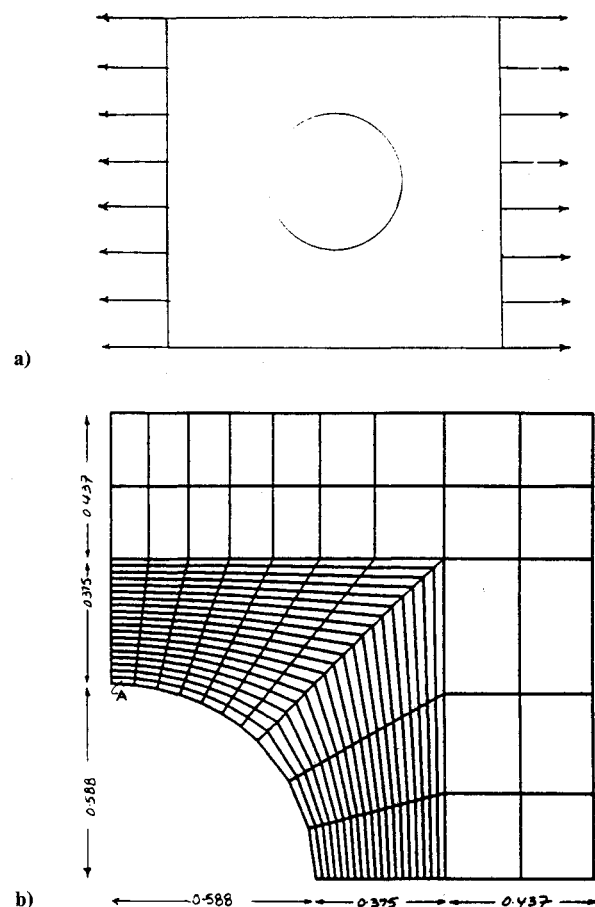


Fig. 1 Plate with a central hole subjected to uniform loading; a) geometry; b) discretization (496 nodes, 214 elements).

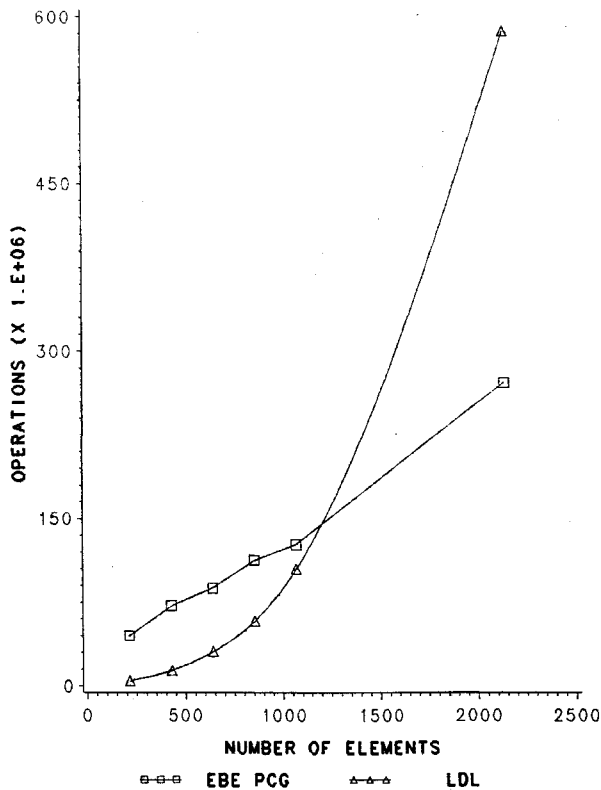


Fig. 2 Number of floating-point operations for LDL^T factorization and EBE PCG iterative solution.

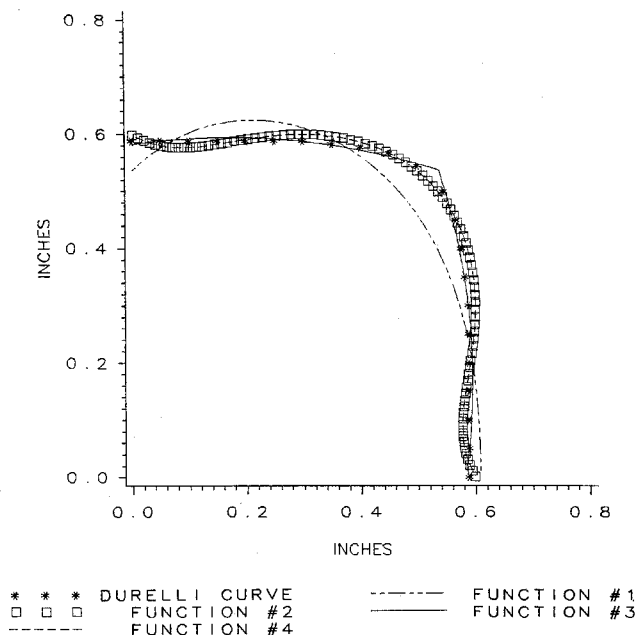


Fig. 3 Three-term least-squares approximation of optimum shape of Durelli and Rajaiah⁷ by the four candidate series.

The number of elements through the thickness of the plate has a large effect on the bandwidth of the global stiffness matrix and therefore influences the relative efficiency of the EBE PCG method vs Gaussian elimination. Table 1 presents a comparison of the convergence of the EBE PCG method for several thickness discretizations of the plate. Columns 1 and 2 present the number of layers and the total number of elements in the model, respectively. Column 3 shows the number of iterations required for the convergence of the EBE PCG. We can see a decrease of the number of iterations as the number of elements is increased. The number of operations per itera-

tion is directly proportional to the number of elements. Column 4 presents the total number of arithmetic operations used in the solution of Eq. (1) for each discretization. Considering now an LDL^T solver, the total number of operations for the decomposition and backsubstitution is proportional to $nN^2/2$, where n and N are the number of degrees of freedom and the bandwidth of the model, respectively (shown in columns 5 and 6). The number of operations are presented in column 7; for the five-layer case the LDL^T solver would require more than 21 times the number of operations than the single-layer case, compared to fewer than 3 for the EBE PCG method. Figure 2 presents the number of operations for both methods vs the number of elements in the model. The LDL^T is very efficient for the one-layer case; however, as the model becomes more three-dimensional, the EBE PCG method becomes more competitive.

The number of elements through the thickness actually needed for good modeling depends on the material properties. For a laminated composite plate we can expect the need for a large number of elements if interlaminar stresses are to be modeled accurately. However, in the present application, because of the isotropy of the experimental specimen⁷ and computational cost considerations, only one layer of through-the-thickness elements was used in most calculations. However, the effect of number of layers was studied at the end by considering a three-layer model.

One of the aspects of the problem was to find a function that would reasonably approximate the hole boundary. Because of the fairly crude model, it was important that the number of design variables needed to represent the boundary be small. Four functions were considered:

$$R = \sum_{i=1}^{nr} R_i \cos^{i-1} \theta \quad (7)$$

$$R = \sum_{i=1}^{nr} R_i \cos \left[(i-1) \left(\theta - \frac{\pi}{4} \right) \right] \quad (8)$$

$$R = \sum_{i=1}^{nr} R_i \sin^{i-1}(\theta') \quad (9)$$

$$\theta' = \theta \quad \text{for } \theta \leq \frac{\pi}{4}; \quad \theta' = \left(\frac{\pi}{2} - \theta \right) \quad \text{for } \theta > \frac{\pi}{4}$$

$$R = \sum_{i=1}^{nr} R_i \left[1 + \cos \left(\theta + 3 \frac{\pi}{4} \right) \right]^{i-1} \quad (10)$$

where R is the radius at a given value of the angular position θ , and R_i are the coefficients in the series. To check which of these series is most appropriate for the optimum design problem, the experimental optimum obtained by Durelli and Rajaiah⁷ was matched by a three-term least-squares approximation with each function, and the results are shown in Fig. 3. The functions given in Eqs. (7–10) are labeled 1–4, respectively, in Fig. 3. It is seen that function 1 is a poor approximation, whereas functions 2–4 can approximate well the Durelli optimum. Based on these results, and some additional experience using functions 2 and 3 in the optimization process (also see the section on optimization results), we selected function 3 (the sine series) to represent the shape of the hole.

The optimization problem is to determine the coefficients R_i (in vector form \mathbf{R}) in order to minimize the maximum Von Mises stress β in the elements of the plate. The optimization problem is formulated with β as an additional design variable as

$$\begin{aligned} &\text{minimize} && \beta \\ &\text{subject to} && \sigma_{\text{von}}(j, \mathbf{R}) \leq \beta, \quad j = 1, \dots, \text{nele} \\ &&& G(\mathbf{R}) \leq 0 \end{aligned} \quad (11)$$

where $\sigma_{\text{von}}(j, \mathbf{R})$ is the Von Mises stress in element j , and nele the number of elements in the plate. $G(\mathbf{R})$ is a set of side

Table 2 Convergence of Von Mises stress (σ_{10}) and stress derivatives in element *A* (see Fig. 1) as a function of number of iterations ($R_1 = 0.5880$ in., $R_2 = 0.01729$ in., $R_3 = 0.1058$ in., $R_4 = 0.2730$ in.)

No. of CG iterations	σ_{10} , psi		$\frac{\partial \sigma_{10}}{\partial R_3}$, lb/in. ³			
			Traditional approach		Correction method [Eq. (13)]	
	$u_0 = u_f^{-1}$	$u_0 = 0$	$u_0 = u_f^{-1}$	$u_0 = 0$	$u_0 = u_f^{-1}$	$u_0 = 0$
30	11,059.8	7,421.89	-13,698	-7099.1	-15,048	-14,643
40	11,004.7	9,978.51	-30,298	-19,286	-13,334	-13,557
50	11,014.8	11,051.2	-13,816	-12,991	-13,381	-13,409
60	11,000.9	11,009.9	-13,575	-13,739	-13,374	-13,360
70	11,006.4	11,022.1	-16,971	-13,168	-13,412	-13,403
100	11,015.8	11,001.2	-14,108	-13,207	-13,379	-13,375

Table 3 Maximum Von Mises stress for the optimum design obtained with candidate functions with increasing number of design variables

Function	nr	σ_{von} , psi
$R = \sum_{i=1}^{nr} R_i \cos^{i-1}(\theta)$	3	13,810
	5	11,770
	7	11,540
	3	12,390
$R = \sum_{i=1}^{nr} R_i \cos[(i-1)(\theta - \pi/4)]$	5	12,030
	7	11,620
$R = \sum_{i=1}^{nr} R_i \sin^{i-1}(\theta')$	3	11,250
$\theta' = \theta$ for $\theta \leq \frac{\pi}{4}$	5	10,830
$\theta' = \left(\frac{\pi}{2} - \theta\right)$ for $\theta > \frac{\pi}{4}$	7	10,830
$R = \sum_{i=1}^{nr} R_i [1 + \cos(\theta + 3\pi/4)]^{i-1}$	3	12,390
	5	11,830
	7	11,750

constraints used to preserve a reasonable geometry, including a limit (from Ref. 7) that the radius is at least 0.588 in. at every hole boundary node.

The optimization problem is linearized and solved by sequential linear programming (SLP). At each design cycle, the optimization problem is linearized with move limits imposed to guarantee the accuracy of the approximation. The constraints and their derivatives are evaluated based on partially converged analysis results. The optimum obtained by the LP program is then used as an initial design for the next optimization, with another partially converged analysis used for the new design.

Partial Convergence and Sensitivity Calculations

A key to the success of the procedure is the choice of number of iterations to be used in the partially converged analysis. This choice affects the accuracy of the structural response, but its most critical effect is on the accuracy of the derivatives of the response with respect to the design variables. The derivatives were calculated by forward finite differences by perturbing each design variable in turn and repeating the analysis for the perturbed design.

Because the EBE PCG analysis solution is iterative, a key question is what should be the initial values of the displacement vector used for the nominal and perturbed designs. For the nominal design it is possible to always start the displacement from the same fixed starting point. In the present work it was found that starting the displacement from zero usually gave satisfactory results. The other option is to start the displacement from zero for the initial design, but for subsequent designs to use the solution of the previous design as a starting point.

For the perturbed design used for derivative calculation we have two different options. First, we can use the same type of initial guess that was used for the displacement vector of the nominal design (e.g., the zero vector). Second, we can use the final iterate of the nominal-design solution. In this second case, however, it is essential to modify the perturbed design equation using the correction method of Ref. 8 in order to prevent errors due to partial convergence. That is, instead of replacing Eq. (1) by

$$(K + \Delta K)u = f + \Delta f \quad (12)$$

we solve

$$(K + \Delta K)u = Ku_0 + \Delta f \quad (13)$$

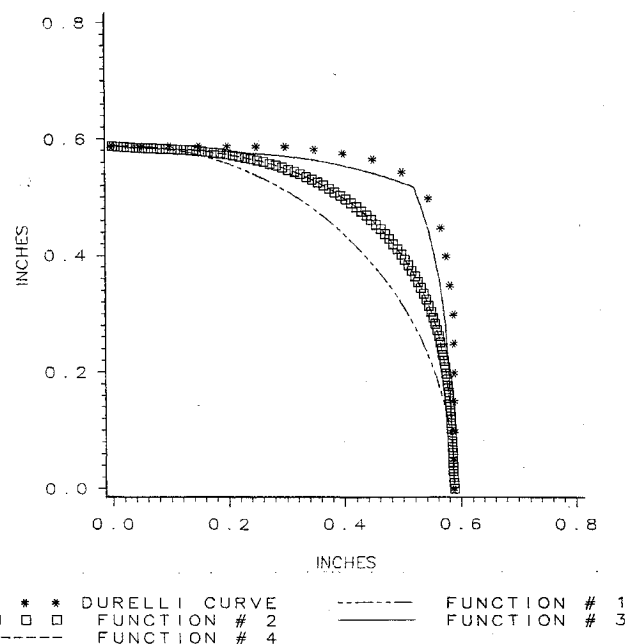
**Fig. 4** Optimum hole shapes obtained by the four candidate series using three terms.

Table 4 Series coefficients (design variables) for optimum designs obtained with sine function (function 3)

nr	R_1	R_2	R_3	R_4	R_5	R_6	R_7	σ_{von} , psi
3	0.58800	-0.03884	0.34690					11,250
5	0.58800	0.03103	-0.01692	0.39600	-0.04979			10,830
7	0.58800	0.01888	0.04651	0.62710	-1.9560	3.6380	-2.1770	10,830

Table 5 Dependence of optimum design on number of analysis (CG) iterations; $u_0 = 0$ (one layer)

No. of CG iterations	R_1	R_2	R_3	σ_{von} Partial convergence, psi	σ_{von} Full convergence, psi	No. of optimization cycles	CPU time, s
30	0.58800	-0.01894	0.16920	10,150	12,900	4	144
40	0.58800	-0.03403	0.30390	11,340	11,640	4	176
50	0.58800	-0.03876	0.34620	11,310	11,300	3	150
70	0.58800	-0.03839	0.34290	11,280	11,290	4	255

Table 6 Dependence of optimum design on number of analysis (CG) iterations; $u_0 = u_f^{-1}$ (one layer)

No. of CG iterations	R_1	R_2	R_3	σ_{von} Partial convergence, psi	σ_{von} Full convergence, psi	No. of optimization cycles	CPU time, s
20	0.58800	-0.03829	0.34200	11,270	11,280	11	323
30	0.58800	-0.03873	0.34590	11,250	11,300	4	149
40	0.58800	-0.03836	0.34260	11,300	11,280	4	178
50	0.58800	-0.03859	0.34470	11,300	11,290	3	155
70	0.58800	-0.03860	0.34480	11,290	11,290	4	266

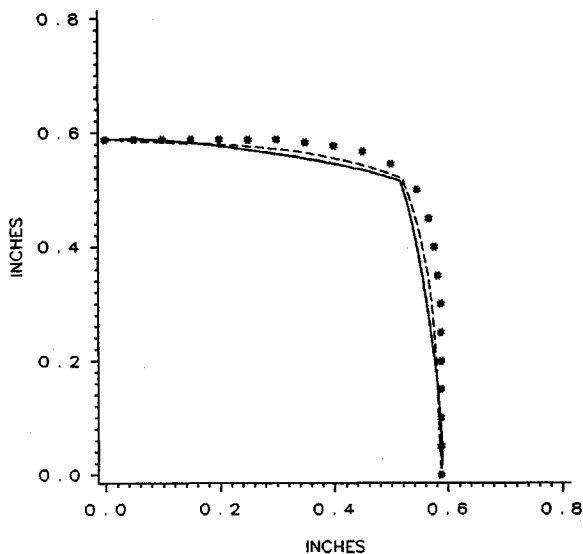


Fig. 5 Optimum hole shapes obtained with sine series (function 3).

where u_0 is the partially converged solution for the nominal design. Note that, when Eq. (13) is used, the solution will tend to u_0 as the perturbation goes to zero. In contrast, if we solved Eq. (12), as the perturbation tends to zero the solution will not tend to u_0 but instead to a more accurate value of the nominal solution and then the finite-difference derivative will tend to infinity.

The various methods for calculating the response and its derivatives were compared after one optimization cycle (i.e., one LP solution), with the results summarized in Table 2. The second column in Table 2 shows the convergence of the highest Von Mises stress in the element marked A (see Fig. 1)

when the initial displacement field iterate is the final iterate u_f^{-1} obtained at the previous (in this case initial) design. The third column presents the same stress obtained with a zero initial displacement field iterate. It is seen that convergence with a zero initial displacement field is inferior to the results obtained with the displacement field of the previous design.

The last four columns in Table 2 compare the convergence of the derivative of the stress with respect to R_3 . The results given in columns 4 and 5 were obtained with the starting point for the perturbed solution paralleling the starting point for the nominal solution. Thus, the results given in column 4 were obtained by starting the perturbed solution from the final iterate of the same perturbed solution for the previous design (with the nominal solution obtained in a similar way). Column 5 represents results with both the nominal and perturbed solutions started from zero. Columns 6 and 7 contain derivatives based on the correction method [Eq. (13)] with the initial iterate for the perturbed design being the final iterate of the nominal solution. Column 6 represents results where the initial solution for the nominal design was started from the final iterate of the solution of the previous nominal design, and column 7 shows results obtained with the nominal solution started from zero.

It is seen that derivatives based on Eq. (13) are more stable and more accurate than the results based on parallel treatment of the nominal and perturbed solutions. Based on these results, a derivative calculation was performed based on Eq. (13). With this approach we did not find any significant difference between the derivative calculated with $u_0 = 0$ and those calculated with $u_0 = u_f^{-1}$.

Optimization Results

The four candidate functions were used in the optimization process with three design variables. The results are summarized in Fig. 4, which compares the optimum shapes with the experimental optimum. Clearly, the sine function (function 3)

Table 7 Dependence of optimum design on number of analysis (CG) iterations; $u_0 = 0$ (three layers)

No. of CG iterations	R_1	R_2	R_3	σ_{von} Partial convergence, psi	σ_{von} Full convergence, psi	No. of optimization cycles	CPU time, s
20	0.58800	-0.02437	0.21770	9258	12,610	5	394
30	0.58800	0.02781	0.14800	9977	11,310	5	488
40	0.58800	-0.03196	0.28540	11,470	11,980	17	1969
50	0.58800	-0.04292	0.38330	11,390	11,360	5	678
70	0.58800	-0.04100	0.35810	11,270	11,320	3	521

Table 8 Dependence of optimum design on number of analysis (CG) iterations; $u_0 = u_f^{-1}$ (three layers)

No. of CG iterations	R_1	R_2	R_3	σ_{von} Partial convergence, psi	σ_{von} Full convergence, psi	No. of optimization cycles	CPU time, s
20	0.58800	-0.04026	0.35950	11,270	11,280	11	865
30	0.58800	-0.04022	0.35920	11,280	11,290	7	684
40	0.58800	-0.04026	0.35960	11,290	11,280	4	467
50	0.58800	-0.04025	0.35950	11,280	11,280	3	405
70	0.58800	-0.04038	0.36070	11,290	11,290	3	519

is the closest. The performance of the four candidate functions, as measured by the maximum Von Mises stress, is shown in Table 3 for increasing number of terms in the series. It is seen that the sine series with three terms outperforms the other series with seven terms. The fast convergence of the series is also evident in Fig. 5, which shows the optimum shapes obtained as the number of terms in the sine series is increased. The figure shows a slight change when the number of design variables increases from three to five, but virtually no change when the number increases from five to seven. It is interesting to note that convergence of the shape does not correspond to convergence of the design variables, which are given in Table 4.

To study the effect of partial analysis convergence on the performance of the optimization procedure, two cases were considered. For the first case the optimization was started from an initial estimate for u_0 equal to zero for each design. This case represents the unintegrated approach. For the second case u_0 was equal to zero for the initial design, but equal to u_f^{-1} thereafter. This case represents the integrated approach. Table 5 summarizes the results for the first case. The first column shows the number of iterations used for each analysis, and the next four columns show the final design and the maximum Von Mises stress predicted by the partially converged analysis. The sixth column shows the fully converged Von Mises stress obtained for the final design, and the last two columns show the number of optimization cycles and the CPU time (IBM/3090) required for the optimization.

It is seen that, when the number of analysis iterations is below 50, the accuracy of the maximum Von Mises stress is not good, and this also slows down the optimization process, which converges more slowly. This indicates that using too few iterations in the analysis is counterproductive. Beyond 50 iterations the CPU time increases again because of the additional cost of each analysis.

The results for the second case where u_0 is taken to be the last iterate of the previous design are summarized in Table 6. The results are much better compared to the case with $u_0 = 0$ presented in Table 5. A good converged estimate for the maximum Von Mises stress can be obtained even for a small number of analysis iterations (20) but at the expense of increasing the number of optimization cycles. The results for 30 analysis iterations are very good. The difference between Tables 5 and 6 is one measure of the effectiveness of the approach of integrating the convergence of the analysis and

design iterations. It appears that the integrated approach reduces the number of analysis iterations needed for convergence from 50 to 30.

The study was then repeated with a three-layer model of the plate, and the results are summarized in Tables 7 and 8. For the unintegrated approach ($u_0 = 0$) very poor accuracy is observed for 20 and 30 iterations. For 40 iterations the accuracy of stresses fluctuated leading to oscillations and poor convergence of the optimizations. As in the one-layer case, the convergence of the integrated design ($u_0 = u_f^{-1}$) was substantially better.

Concluding Remarks

The optimum design of the shape of a hole in a plate in tension was obtained with a design algorithm that integrates the convergence of the analysis and design iterations. The plate was modeled by three-dimensional finite elements, and the EBE PCG iterative solution algorithm was used for solving the equations of equilibrium. Several parametrizations of the optimum shape were considered, and it was found that a sine series could describe the optimum shape with only three design variables, whereas other series required seven variables for similar results. The optimum shape compared well with an experimental optimum obtained by Durelli and Rajaiah.⁷

An investigation was performed to determine the best way of obtaining finite-difference derivatives of the stresses with respect to design variables. It was found that a method based on modifying the equations of equilibrium solved by the perturbed solution performed best. The benefit of the integrated approach was determined by comparing convergence with different initial iterates for the displacement field. It was found that using the final iterate of the previous solution can reduce the number of analysis iterations by about 40% compared to starting with a zero initial iterate.

Acknowledgment

This research was supported by NASA Grant NAG-1-168.

References

- 1Fox, R. L., and Schmit, L. A., "Advances in the Integrated Approach to Structural Synthesis," *Journal of Spacecraft and Rockets*, Vol. 3, June 1966, pp. 858-866.
- 2Hughes, T. J. R., Levit, I., and Winget, J. M., "An Element-by-

Element Solution Algorithm for Problems of Structural and Solid Mechanics," *Computer Methods in Applied Mechanics and Engineering*, Vol. 36, Feb. 1983, pp. 241-254.

³Hughes, T. J. R., Levit, I., Winget, J. M., and Tezduyar, T., "New Alternating Direction Procedures in Finite Element Analysis Based upon EBE Approximate Factorizations," *Computer Methods for Nonlinear and Structural Mechanics*, Vol. 4, edited by S. N. Atluri and N. Perrone, 1983, pp. 79-109.

⁴Haftka, R. T., "Simultaneous Analysis and Design," *AIAA Journal*, Vol. 23, No. 7, 1985, pp. 1099-1103.

⁵Haftka, R. T., and Kamat, M. P., "Simultaneous Nonlinear

Structural Analysis and Design," *Computational Mechanics*, Vol. 4, No. 6, 1989, pp. 409-416.

⁶Rizk, M. H., "The Single-Cycle Scheme—A New Approach to Numerical Optimization," *AIAA Journal*, Vol. 21, Dec. 1983, pp. 1640-1647.

⁷Durelli, A. J., and Rajaiah, K., "Optimum Hole Shapes in Finite Plates Under Uniaxial Load," *Journal of Applied Mechanics*, Vol. 46, Sept. 1979, pp. 691-695.

⁸Haftka, R. T., "Sensitivity Calculations for Iteratively Solved Problems," *International Journal for Numerical Methods in Engineering*, Vol. 21, Aug. 1985, pp. 1535-1546.

*Recommended Reading from the AIAA
Progress in Astronautics and Aeronautics Series . . .*



Thermal Design of Aeroassisted Orbital Transfer Vehicles

H. F. Nelson, editor

Underscoring the importance of sound thermophysical knowledge in spacecraft design, this volume emphasizes effective use of numerical analysis and presents recent advances and current thinking about the design of aeroassisted orbital transfer vehicles (AOTVs). Its 22 chapters cover flow field analysis, trajectories (including impact of atmospheric uncertainties and viscous interaction effects), thermal protection, and surface effects such as temperature-dependent reaction rate expressions for oxygen recombination; surface-ship equations for low-Reynolds-number multicomponent air flow, rate chemistry in flight regimes, and noncatalytic surfaces for metallic heat shields.

TO ORDER: Write, Phone or FAX:

American Institute of Aeronautics and Astronautics,
c/o TASC0, 9 Jay Gould Ct., P.O. Box 753, Waldorf, MD 20604
Phone (301) 645-5643, Dept. 415 ■ FAX (301) 843-0159

Sales Tax: CA residents, 7%; DC, 6%. For shipping and handling add \$4.75 for 1-4 books (call for rates for higher quantities). Orders under \$50.00 must be prepaid. Foreign orders must be prepaid. Please allow 4 weeks for delivery. Prices are subject to change without notice. Returns will be accepted within 15 days.

**1985 566 pp., illus. Hardback
ISBN 0-915928-94-9**

AIAA Members \$54.95

Nonmembers \$81.95

Order Number V-96